Journal of proteome research

Article

pubs.acs.org/jpr

Global Metabolomic and Isobaric Tagging Capillary Liquid Chromatography–Tandem Mass Spectrometry Approaches for Uncovering Pathway Dysfunction in Diabetic Mouse Aorta

Laura A. Filla,[†,⊥] Wei Yuan,[⊥,‡,§] Eva L. Feldman,[∥] Shuwei Li,[‡,§] and James L. Edwards*[,†]

[†]Department of Chemistry, Saint Louis University, St. Louis, Missouri 63103, United States

[‡]Institute for Bioscience and Biotechnology Research, 9600 Gudelsky Drive, Rockville, Maryland 20850, United States

[§]Department of Chemistry and Biochemistry, University of Maryland, College Park, Maryland 20742, United States

[∥]Department of Neurology, University of Michigan, Ann Arbor, Michigan 48109, United States

Supporting Information

ABSTRACT: Despite the prevalence of diabetes and the global health risks it poses, the biochemical pathogenesis of diabetic complications remains poorly understood with few effective therapies. This study employs capillary liquid chromatography (capLC) and tandem mass spectrometry (MS/MS) in conjunction with both global metabolomics and isobaric tags specific to amines and carbonyls to probe aortic metabolic content in diabetic mice with hyperglycemia, hyperlipidemia, hypertension, and stenotic vascular damage. Using these combined techniques, metabolites well-characterized in diabetes as well as novel pathways were investigated. A total of 53 986 features were detected, 719 compounds were identified as having significant fold changes (thresholds ≥2 or ≤0.5), and 48 metabolic pathways were found to be altered with at least 2 metabolite hits in diabetic samples. Pathways related to carbonyl stress, carbohydrate metabolism, and amino acid metabolism showed the greatest number of metabolite changes. Three novel pathways with previously limited or undescribed roles in diabetic complications—vitamin B6, propanoate, and butanoate metabolism—were also shown to be altered in multiple points along the pathway. These discoveries support the theory that diabetic vascular complications arise from the interplay of a myriad of metabolic pathways in conjunction with oxidative and carbonyl stress, which may provide not only new and much needed biomarkers but also insights into novel therapeutic targets.

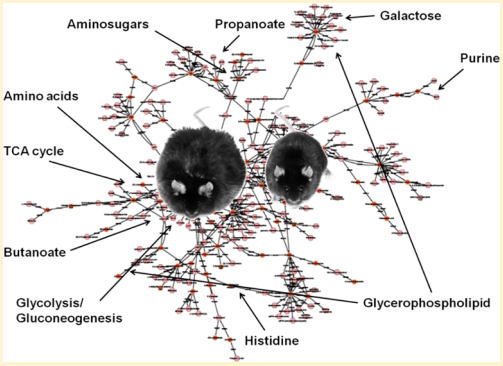

KEYWORDS: *diabetes, diabetic complications, global metabolomics, isobaric tags, capillary liquid chromatography, tandem mass spectrometry, metabolic pathway dysfunction*

INTRODUCTION

Diabetes is a chronic metabolic disorder characterized by the inability to effectively produce or use insulin, resulting in hyperglycemia and enhanced lipolysis. Perturbations in both glucose and lipid metabolism contribute to the production of reactive oxygen species (ROS) by the mitochondrial electron transport chain, which diminish production of the vasodilator nitric oxide (NO) and impair vascular function.[1] Vascular tissue is susceptible to hyperglycemic damage due to its inability to regulate intracellular glucose levels.[2] Hypertension frequently accompanies and accelerates the development of stenotic cardiovascular disease, which is responsible for 80% of deaths in patients with diabetes.[3,4] Oxidative stress promoted by hyperglycemia and hyperlipidemia causes diabetic tissue damage through several metabolic pathways, including increased polyol pathway flux and the formation of advanced glycation end products (AGEs).[1] Current therapies targeting these pathways have proven ineffective in the long-term prevention of vascular injury. Identifying alternate metabolic aberrations in diabetic vascular tissue is thus crucial to understanding the relationship between hyperglycemia, associated dyslipidemia, and vascular damage in order to establish novel therapeutic targets.

Functional genomics and proteomics can increase our understanding of the pathophysiology of diabetes. However, examination of a single class of molecules will inevitably restrict the discovery of novel pathways and mechanisms. Global analyses of genes, gene expression, and proteins have shown over 2 million biochemical changes often implicating metabolic pathways.[5,6] For instance, a proteomics profiling study investigating human pancreatic islets classified 25% of the isolated proteins as having a role in cell metabolism.[7] This supports our contention that metabolomic strategies are needed to complement proteomic and genomic findings.

Received: October 13, 2014
Published: November 4, 2014

   dx.doi.org/10.1021/pr501030e | J. Proteome Res. 2014, 13, 6121−6134

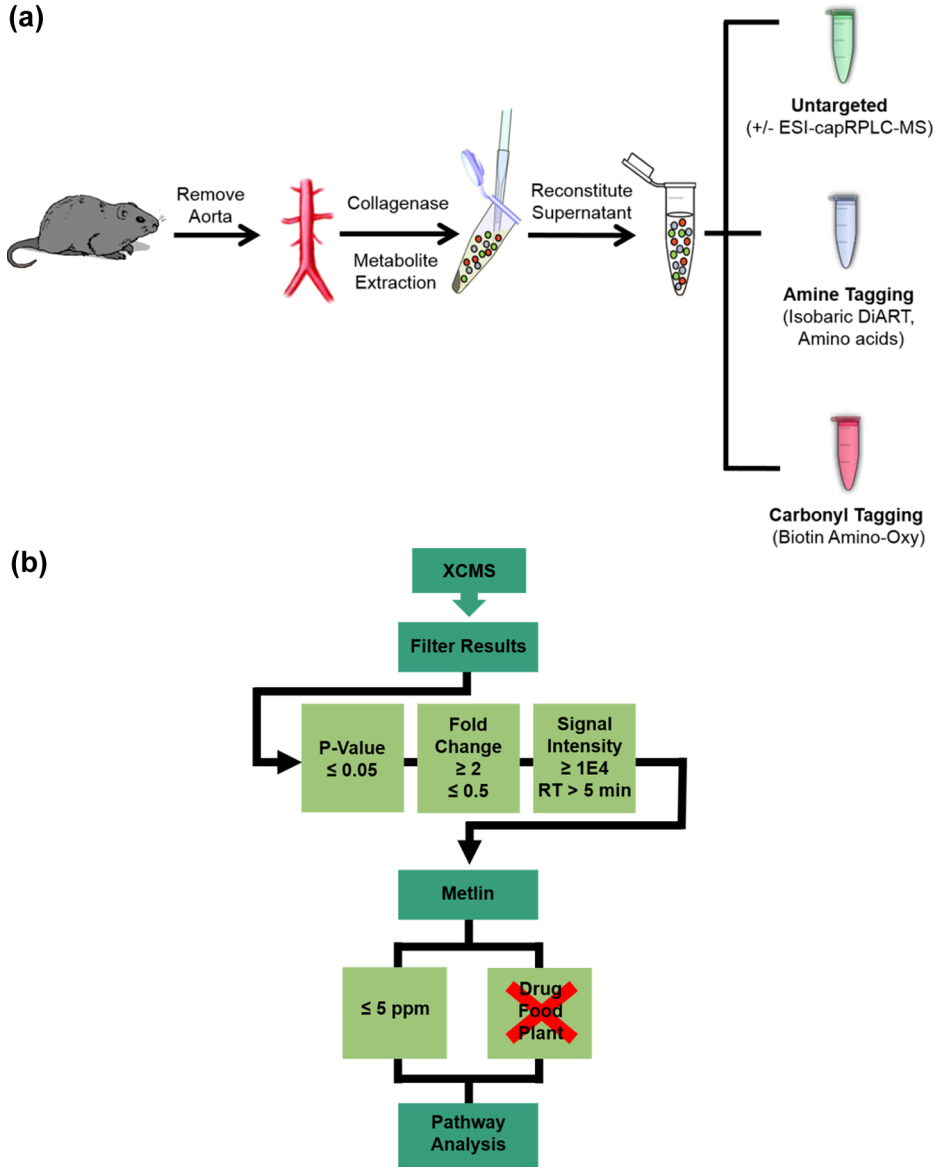

Figure 1. (a) Schematic of sample preparation. Aortas are removed from either *db*/*db* or *db*/+ mice and digested with collagenase. Cell lysis is accomplished using 80% MeOH and a sonic dismembrator. Samples are centrifuged and metabolites are dried and reconstituted in 30 μL of H_2O/formic acid. Analysis is accomplished by four different modes: positive and negative untargeted, semitargeted amine tagging, and semitargeted carbonyl tagging. (b) Untargeted positive and negative mode data analysis flowchart. Analysis steps (dark green) include XCMS, filtering resulting peaks, identification using METLIN, and pathway analysis with MetPA. Criteria for data processing (light green) consists of fold change, *p*-value, retention time, and signal intensity thresholds. Nonendogenous metabolites and peaks with *m*/*z* greater than 5 ppm are excluded from results.

Liquid chromatography−mass spectrometry (LC−MS) is used to elucidate metabolic signatures of vascular damage by analyzing cultured cells and plasma.[8,9] Such investigations report a correlation between advanced glycation end products, branched chain amino acids, and macrovascular disease.[10,11] LC−MS based metabolomics of vascular tissue reveals an interplay between metabolic pathways and external stimuli such as surgery or hyperlipidemic diet.[12,13] Although these findings yield useful biomarkers for vascular dysfunction, the metabolic connections between these compounds, particularly with regard to diabetic complications, remain unclear.

Despite the relationship between abnormal glucose and lipid metabolism and aortic damage, few studies attempt to identify the metabolic pathways that become defective in vascular dysfunction, in part due to the lack of sensitivity, selectivity, and quantitation in metabolomic strategies. Isotope-labeling approaches can overcome these limitations by improving quantitation and selecting classes of metabolites for analysis.[14] We have described a cleavable isobaric labeling affinity tag (CILAT) for the selective enrichment of carbonyls from a biological sample.[15] As aldehydes and ketones are implicated in diabetic pathogenesis,[16] these tags make it possible to highlight carbonyl stresses within aortic tissue. Also employed in this study is a deuterium isobaric amine reactive tag (DiART), which is used to selectively tag amines.[17] The DiART tag offers a 100-fold signal-to-noise enhancement in mass spectrometry analyses of amines. We also describe here a global approach to identifying metabolites that change in response to hyperglycemia based on both exact mass and MS/MS fragmentation. In this study, we employ both targeted and untargeted approaches to examine multiple classes of metabolites in harvested diabetic and control mice aorta. All experiments are

dx.doi.org/10.1021/pr501030e | *J. Proteome Res.* 2014, 13, 6121−6134

conducted in a capillary LC (capLC) column, which provides an additional level of sensitivity over conventional bore HPLC techniques.[18] Using these combined approaches, we report significant changes in 719 compounds present in 48 metabolic pathways in diabetic vascular tissue.

MATERIALS AND METHODS

Materials

Triethylammonium bicarbonate buffer (1 M, pH 8.5) and aniline were obtained from Sigma-Aldrich (St. Louis, MO). DiART 6-plex reagents and CILAT 2-plex reagents were synthesized in-house.[15,19] HPLC-grade solvents were purchased from Honeywell Burdick & Jackson (Muskegon, MI). 4-[3-(Perfluorooctyl)-propyl-1-oxy]benzaldehyde was obtained from Fluorous Technologies Inc. (Ambridge, PA). Strepavidin Sepharose high-performance beads were purchased from GE Healthcare Life Sciences (Pittsburgh, PA). Diabetic (BKS.Cg-$m^{+/+}Lepr^{db}$/J, BKS-*db*/*db*) and control (BKS-*db*/+) mice were purchased from Jackson Laboratories (Bar Harbor, ME). Mice were housed in a pathogen-free environment, with continuous access to food (Purina 5053 chow) and water on a 12 h light−12 h dark schedule, and cared for following the University of Michigan Committee on the Care and Use of Animals guidelines (approval no. 07675).[20]

Experimental Methods

A schematic approach for preparation of mice aortic cells for metabolomics studies is illustrated in Figure 1a. Aortas were harvested from the *db*/+ or *db*/*db* mice. After weighing and washing with warm phosphate-buffered saline (PBS), the aortic tissue sample was added to 100 μL of PBS buffer containing collagenase (2 mg/mL) and glucose (*db*/+, 163.5 mg/dL; *db*/*db*, 448 mg/dL).[21] The amount of glucose coincubated with collagenase was determined by the average blood glucose level measured from *db*/+ or *db*/*db* mice at 12 weeks. Following incubation at 37 °C for 15 min, 400 μL of ice-cold methanol was added to quench the collagenase reaction. After resting in a dry ice/ethanol bath for 5 min, the aortas were lysed by sonicating (Mixonix XL-2000, Qsonica, CT) on ice with 10 1-s bursts at low power. Cell lysates were centrifuged at 14 000 rpm for 8 min at 4 °C. The supernatants were collected, dried by SpeedVac, and then reconstituted in 30 μL of H_2O/formic acid.

For untargeted metabolomics analyses, the reconstituted samples were directly subjected to LC−MS analysis in both negative and positive mode. To enrich the amine-containing metabolites, DiART reagents were used as described in previous studies.[17] In brief, 10 μL of the reconstituted sample from *db*/+ or *db*/*db* mouse was added with an excess amount of DiART (114−119) in 70% acetonitrile. For each set of DiART isobars (114−119), three were used to label *db*/+ cell lysates and the other three were used with *db*/*db* cell lysates. The reaction pH was adjusted to 8.5 with triethylammonium bicarbonate (1 M). The labeling reaction was conducted at room temperature for 2.5 h. A set of six samples labeled by DiART 114−119 was mixed at a 1:1 ratio after normalizing to the mass of the mouse aorta from which the aortic cells were obtained. The mixed samples were then dried by SpeedVac.

To label the carbonyls, the reconstituted cell lysates were incubated with 20 mM CILAT 114 (*db*/*db*) or 115 (*db*/+) in 70% acetonitrile containing triethylammonium bicarbonate using aniline (100 mM) as catalyst, as described previously.[15] The pH of the reaction solution was adjusted to 4.5 by 2 M acetic acid. The labeling reactions were conducted for 22 h at 65 °C. Following labeling, the CILAT 114 (*db*/*db*) and 115 (*db*/+) labeled cell lysates were mixed at a 1:1 ratio after normalizing to the mass of the aorta. Excess CILAT tag was scavenged by 4-[3-(perfluorooctyl)-propyl-1-oxy]benzaldehyde. The labeled carbonyls were then captured by streptavidin beads. After UV (365 nm) cleavage, the released CILAT-labeled carbonyls were dried by speedvac.

LC−MS Conditions

LC−MS analyses were performed in positive ion mode (amine metabolites and carbonyls) or both positive and negative mode (untargeted) with a Thermo LTQ Orbitrap Discovery ion trap mass spectrometer (San Jose, CA) equipped with a nanospray ionization (NSI) interface coupled with an Agilent 1200 HPLC (Palo Alto, CA). A microcross (Upchurch, Oakharbor, WA) was placed between the pump and capillary column to reduce the flow rate directed to the capillary column to 20−30 nL/min using a 75 μm i.d. silica capillary as the flow splitter. Separations were performed on 50 μm i.d. silica capillary (Polymicro Technologies, Phoenix, AZ) columns with in-house-made frits packed with 3 μm Atlantis T3 C18 aqueous reverse phase particles (Waters, Milford, MA). All columns had a 20 cm packed bed length.

For analysis of carbonyl and amine metabolites, mobile phase A was 10 mM formic acid in H_2O and mobile phase B was 10 mM formic acid in methanol. Analytes were eluted with a 40 min gradient: 30 min from 0 to 70% solvent B and 10 min from 70 to 95% solvent B. The temperature of the heated MS inlet capillary was 200 °C. Fragmentation was activated by higher-energy collision induced dissociation (HCD) with a collision energy of 45%. All metabolites were analyzed using data-dependent analysis at a resolving power of 15 000. The chromatography and correlation function were activated during data-dependent analysis.

A pH gradient was used for untargeted metabolite analysis. Mobile phase A was 5 mM ammonium formate in H_2O (pH 6), mobile phase B was 10 mM formic acid in H_2O (pH 3), and mobile phase C was 5 mM ammonium formate in methanol. The separation was initiated with 5 min isocratic 100% B followed by a 10 min pH gradient from 100% B to 100% A. The separation was further performed with mobile phase A and C: a 10 min gradient from 0 to 40% C followed by 5 min from 40% C to 90% C. The temperature of the heated MS inlet capillary was 200 °C. Fragmentation was activated by collision-induced dissociation (CID) with a collision energy of 35%. All metabolites were analyzed using data-dependent analysis at a resolving power of 30 000.

The instrument control, data acquisition, and data analysis were performed by Xcalibur software (Thermo Electron Corporation, version 2.0.7 SP1). The quantification of DiART-labeled amines and CILAT-labeled carbonyls was processed with an in-house-written program.

Data Analysis

Untargeted Positive and Negative Mode. Xcalibur untargeted data files from each control (n = 5) and diabetic (n = 6) sample were analyzed using the Scripps Center for Metabolomics data processing program XCMS Online.[22] Each signal was normalized to aorta mass, and median m/z ratios and median retention times were obtained. Fold change was determined by dividing the average *db*/*db* signal by the average *db*/+ signal. A two-tailed Student's t test was performed on *db*/*db* and *db*/+ sample groups. Any peaks with p-value ≥0.05 or

dx.doi.org/10.1021/pr501030e | J. Proteome Res. 2014, 13, 6121−6134

fold change ≤2 for increases and ≥0.5 for decreases were excluded from further analysis. The remaining peaks were further processed by rejecting peaks with retention times of less than 5 min (the dead time of unretained species) and signal intensity below 1E4.

The Scripps Center for Metabolomics database METLIN[23] was used to find metabolites (adducts +H for positive mode and −H for negative mode) that match m/z ratios of the remaining peaks within ±5 ppm. Nonendogenous metabolites were excluded from these results on the basis of their origin classification in the Human Metabolome Database (HMDB);[24] ID numbers from the database Kyoto Encyclopedia of Genes and Genomes (KEGG)[25] were obtained where available. Over-representation and pathway topological analyses were conducted with hypergeometric and relative-betweenness centrality algorithms using the visualization tool Metabolomics Pathway Analysis (MetPA).[26] Only pathways with two or more metabolite hits were reported. The overall data analysis scheme is outlined by Figure 1b.

Each peak with an exact mass identification was further processed for structural information by comparing MS/MS spectra using the appropriate scan filter in Xcalibur with fragmentation patterns of standards in METLIN. Where database MS/MS spectra were not available, manual MS/MS identifications were performed. Cases in which MS/MS structural information did not match the compound proposed by METLIN were noted; these are potentially unknown metabolites not previously characterized or detected.

Carbonyl (CILAT) Data. Data sets of pooled *db/db* (CILAT 114) and *db/+* (CILAT 115) samples (n = 4) were processed using XCMS Online. The compound masses obtained from the four data sets were grouped, and masses within ±0.01 Da that had retention times within 5% RSD were considered to be the same compound. Only compounds detected in at least three of the four analyses were marked for identification. In some cases, peaks were picked multiple times within the same sample. Average masses of these duplicate peaks were taken and then averaged against the rest of the samples to obtain an overall mean compound mass; this leads to variability in the accurate mass. Of the hits that were generated, only those compounds with carbonyl groups matching the number of tags were chosen for identification.

Theoretical masses were determined by adding the exact mass of the identified metabolite as listed in KEGG to the mass of the tag (372.237 71 Da) multiplied by the charge. Only metabolites with a mass tolerance within 60 ppm were reported. The expanded mass tolerance is due to the increased variance supplied by the tag as well as m/z averaging over four sample sets. The tagged carbonyl compounds were fragmented by data-dependent MS/MS scans to yield the low mass reporter ion. Ratios of 114:115 signal intensities were obtained for each peak and averaged among the four samples to give the average fold change. Fold changes greater than 2.0 or less than 0.5 were used as the threshold for significant change.

Finally, the masses that had significant fold changes and that were detected in at least three of the samples were processed using the database MyCompoundID (MCID). MCID searches for both human metabolites and their predicted products from metabolic reactions.[27] Because alcohols can be oxidized to form aldehydes and ketones (Figure 2)[28] and oxidative stress is implicated in diabetes, we chose to analyze the peaks for dehydrogenation reactions that could produce aldehyde or keto groups that would subsequently be tagged and detected. Only compounds with a number of hydroxyl groups greater than or equal to the number of tags were chosen.

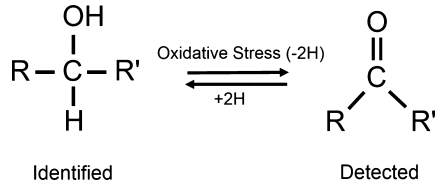

Figure 2. Mechanism of aldehyde and ketone formation from oxidized alcohols. This reaction was selected in MyCompoundID for identification of alcohols that could be oxidized and tagged in the carbonyl studies.

Amine (DiART) Data. *db/+* (n = 5) And *db/db* (n = 6) aortas were treated with DiART tags and compared using two sets of reagents in order to accommodate the total number of samples. Relative fold change and standard deviation were determined using averaged signal intensity.

RESULTS

Metabolomics is capable of revealing metabolic profiles associated with diabetes.[29] This study aims to provide a comprehensive picture of metabolic dysfunction in diabetic aortic tissue by highlighting pathway changes using both functional group tagging and untagged approaches (Figure 1a). Identifying these changes is crucial to understanding the pathogenesis of diabetic vascular complications.

Untagged Global Metabolomic Studies

In a discovery-based LC−MS metabolomics experiment, untargeted or unknown metabolic compounds are surveyed by analyzing all statistically significant chromatographic peaks obtained from a sample.[30] Aortic tissue from control and diabetic samples was analyzed using both positive and negative mode capLC−NSI-MS/MS; 53 986 mass spectral peaks were uncovered using XCMS data processing. Figure 3a,b depicts these data in the form of volcano plots.[31] For the sake of feasibility, a subset of the statistically significant untargeted data was chosen for further analysis, and 8.1% of negative mode peaks and 10.6% of positive mode peaks fell in the statistically significant regions ($p \leq 0.05$ and fold change ≤0.5 or ≥2).[32] The data were further filtered to eliminate peaks with low signal intensity and retention times before the dead time based on the criteria outlined in the Materials and Methods section. This approach reduced the number of features analyzed from 17 248 to 1140 and from 36 738 to 3138 for negative and positive mode data, respectively (Table 1).

METLIN was used to analyze statistically significant features based on exact mass within 5 ppm. HMDB and KEGG were used to identify masses and eliminate compounds not endogenous to mammals (see Materials and Methods section). In virtually all cases, multiple database identification hits obtained from a single mass were attributed to structural isomers. MS/MS fragmentation patterns were used to eliminate structural isomers when possible, although many of these compounds are indistinguishable without further analyses.[33] A total of 174 compounds (72 unique masses) were identified in negative mode, corresponding to 5.1% of statistically relevant compounds. In positive mode, 335 compounds, or 152 unique masses, were identified (4.5% of statistically relevant compounds).

Each compound identified by exact mass was further investigated for structural information by comparing MS/MS

dx.doi.org/10.1021/pr501030e | J. Proteome Res. 2014, 13, 6121−6134

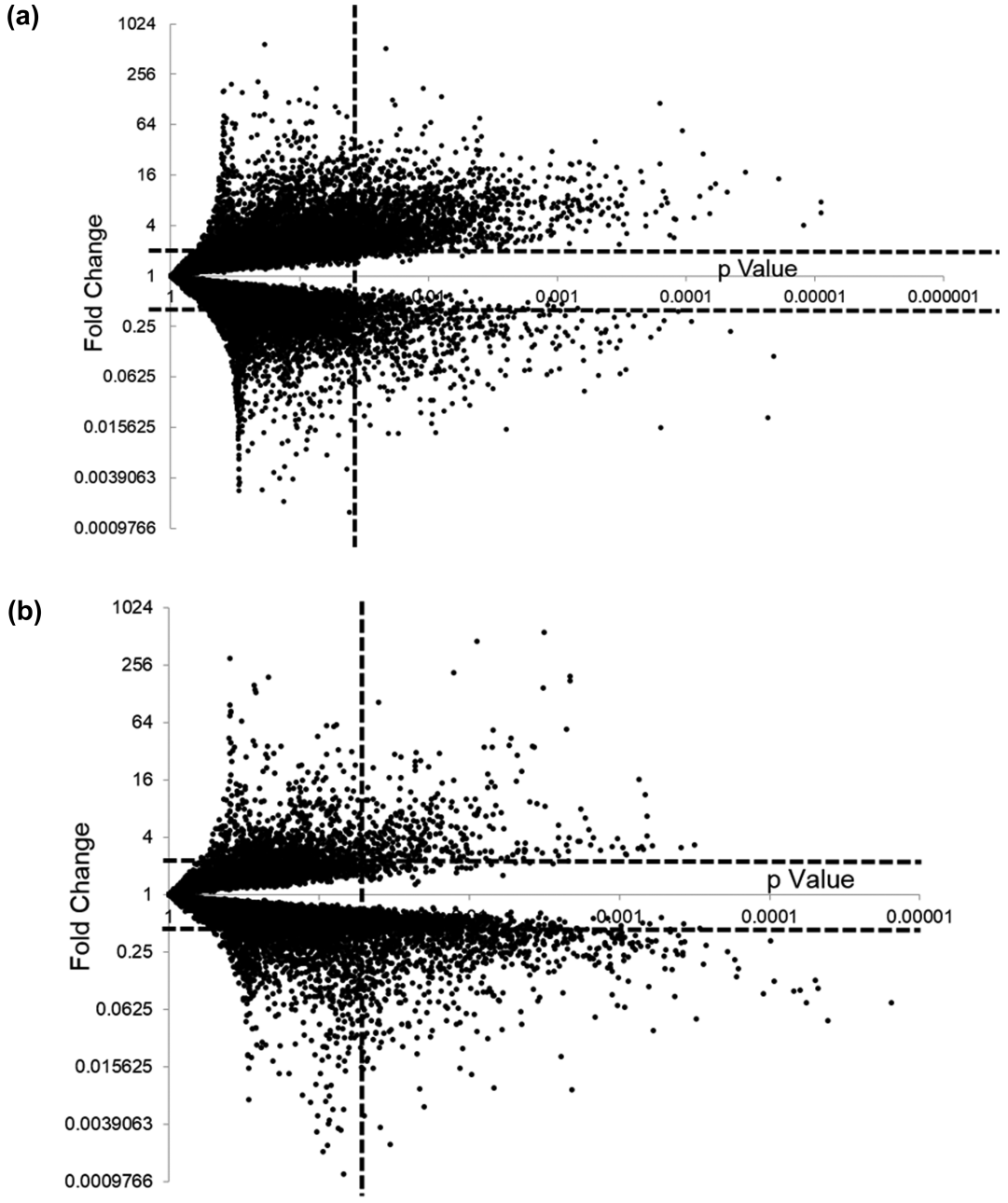

Figure 3. (a) Positive mode volcano plot generated from XCMS data normalized to aorta mass. A total of 36 738 peaks are plotted, with 3346 having a *p*-value ≤0.05 and a fold change ≤0.5 or ≥2. *p*-Values are represented on a $\log_{10}$ scale and fold changes are represented on a $\log_2$ scale. (b) Negative mode volcano plot generated from XCMS data normalized to aorta mass. A total of 17 248 peaks are plotted, with 1401 having a *p*-value ≤0.05 and a fold change ≤0.5 or ≥2. *p*-Values are represented on a $\log_{10}$ scale and fold changes are represented on a $\log_2$ scale.

Table 1. Number of Untargeted Positive and Negative Mode Features Resulting from Each Data Processing Step

	positive mode	negative mode
XCMS Total	36738	17248
$p \leq 0.05$	3582	1897
fold change ≤0.5 or ≥2	3344	1401
signal intensity ≥ 1E4 and t_R > 5 min	3138	1140
METLIN hits	152	72
pathways activated in MetPA	40	39

fragmentation patterns to MS/MS spectra of metabolite standards in the METLIN database. Eight negative mode and 16 positive mode compounds were matched to fragmentation spectra in METLIN (Tables S1 and S2, Supporting Information), corresponding to 11.1% and 10.5% of identifications in negative and positive mode, respectively. These results are consistent with the METLIN compound library itself, which consists of 240 478 metabolites, 4.9% of which have MS/MS spectra.[34]

Untagged Targeted Metabolomic Studies

Negative mode targeted analysis was undertaken for specific pathways expected to be altered by hyperglycemia. Figure 4 shows the metabolites that were targeted in glycolysis and the tricarboxylic acid (TCA) cycle. Metabolites increased with statistical significance through all of glycolysis and the first half of the TCA cycle before succinate. The targeted compounds

dx.doi.org/10.1021/pr501030e | J. Proteome Res. 2014, 13, 6121−6134

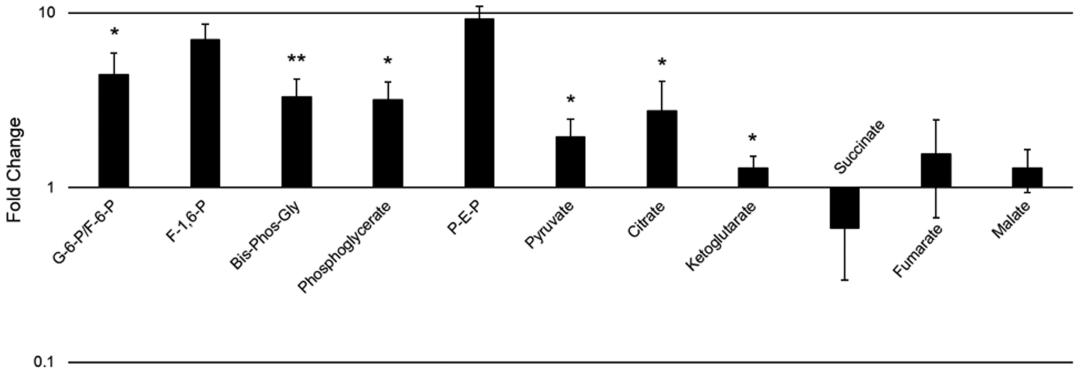

Figure 4. Targeted metabolites in glycolysis and TCA pathways based on matching retention time, exact mass, and MS/MS to standards. The *y*-axis is a logarithimic scale showing fold changes (*db*/*db*:*db*/+) of each metabolite. Error bars are SEM * denotes $p < 0.05$, **denotes $p < 0.01$.

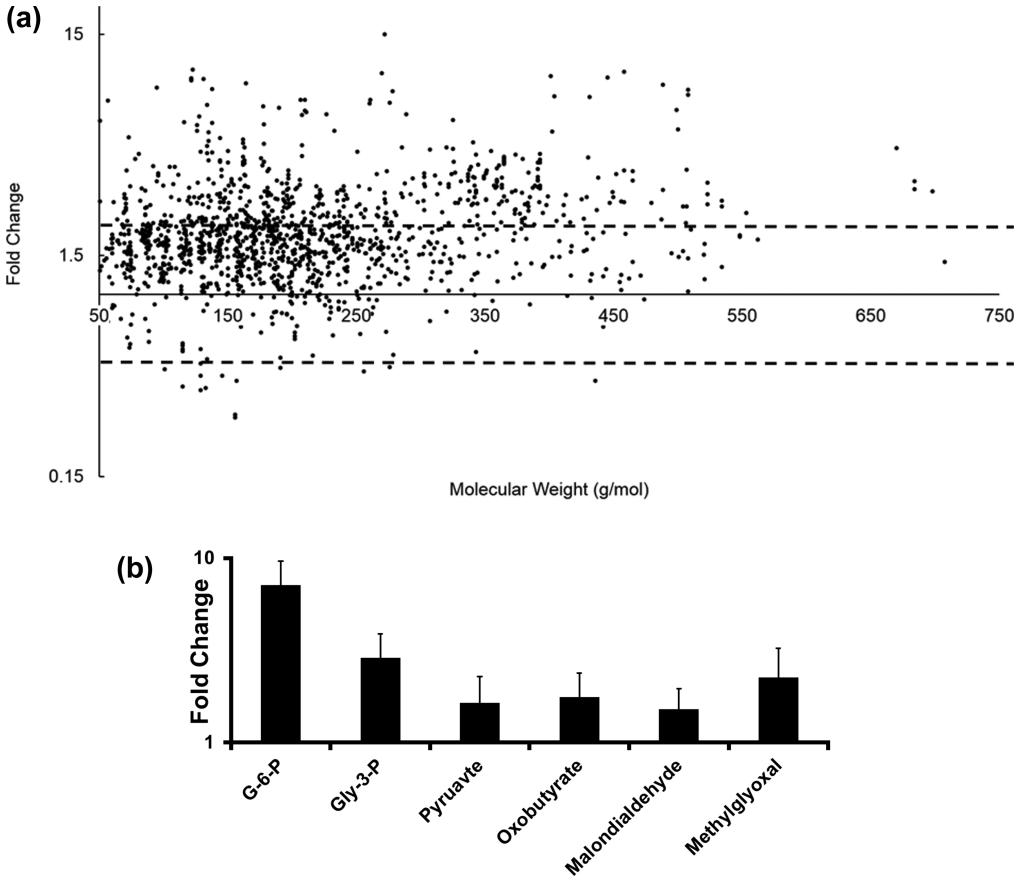

Figure 5. (a) Carbonyl scatter plot showing all peaks detected in CILAT sample B. Dashed lines show cutoffs for fold changes <0.5 and >2. (b) Targeted carbonyl compounds on the basis of matching retention time and exact mass to CILAT-tagged standards. Fold changes are represented on a $\log_{10}$ scale (*db*/*db*:*db*/+) of each metabolite. Error bars are SEM.

with the largest fold changes included phosphoenol-pyruvate (P-E-P) and fructose-1,6-bisphosphate (F-1,6-P), with fold changes of 9.19 and 7.02, respectively. Fructose-6-phosphate/glucose-6-phosphate (F-6-P/G-6-P), bisphosphoglycerate (Bis-Phos-Gly), phosphoglycerate, and citrate had fold changes >2. Six of the targeted metabolites had $p < 0.05$, with one having $p < 0.01$ (Figure 4).

Carbonyl Tagging (CILAT)

Carbonyls were analyzed using a semitargeted approach using CILAT. CILAT allows for the selective enrichment of carbonyls from a sample by purification with photocleavable biotin and ionization enhancement with a tertiary amine tag.[15] *db*/+ (n = 4) And *db*/*db* (n = 4) aorta samples were labeled with CILAT 114 and CILAT 115, respectively, pooled, and analyzed by +NSI-MS/MS. Data analysis was conducted as described in Materials and Methods. Figure 5a shows a scatter plot of all peaks (114/115 ratio) found in one of the samples; almost 12-fold more increases than decreases were detected in this sample. Using METLIN for identifications, a total of 36 compounds increased (97 including isomers) and 2 compounds decreased (4 including isomers, see Tables S3 and S4, Supporting Information).

A carbonyl targeted approach was also taken by selecting parent masses of seven carbonyl compounds known to be of

dx.doi.org/10.1021/pr501030e | *J. Proteome Res.* 2014, 13, 6121−6134

importance in diabetes[16,35] for fragmentation and matching the peaks to retention time and mass of CILAT-tagged commercially available standards. As expected, all but one of the targeted carbonyl compounds increased in the diabetic samples, with G-6-P, glyceraldehyde-3-phosphate (Gly-3-P), and methylglyoxal having fold changes greater than 2 (Figure 5b).

The carbonyl data were also analyzed for alcohols that could be oxidized to form carbonyls that would subsequently be tagged and detected (Figure 2). To accomplish this, masses of untagged compounds were input into the database MyCompoundID, which enables the user to search for metabolites that can undergo various reactions to yield the target mass. In this study, compounds that could be endogenously oxidized (−2H) to produce an aldehyde or ketone and also had hydroxyl groups that matched the number of CILAT tags were chosen for identification (Figure 2). As shown in Tables S5 and S6 (Supporting Information), this investigation produced 88 metabolites with significant increases (25 unique masses) and 6 with significant decreases (5 unique masses).

Amine Tagging (DiART)

The involvement of amino acid metabolism in diabetes has been shown but not fully correlated with other pathways, particularly in tissue. To this end, DiART, an amine specific isobaric tag, was used.[17] *db/db* (n = 6) And *db/+* (n = 5) samples were tagged with DiART 114−119, pooled, and analyzed by separate chromatographic runs. Amino acid parent masses were targeted for fragmentation, and 14 were shown to increase in diabetes (Figure 6). Of these, tyrosine (Tyr), methionine (Met), leucine (Leu), and tryptophan (Trp) had statistically significant p-values. DiART was not performed in untargeted mode due to the overwhelming number of small peptides and protein degradation products present in tissue samples.[36]

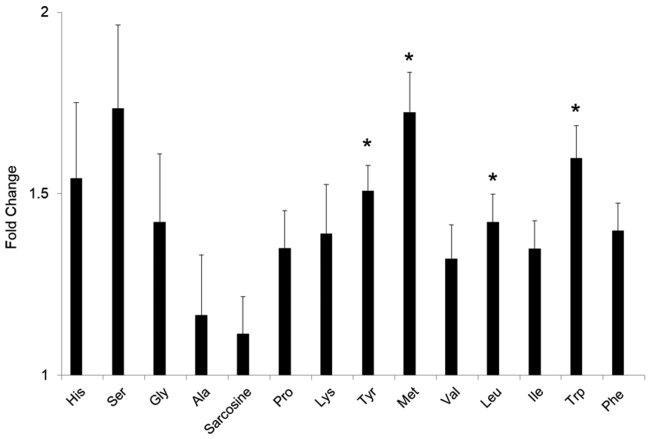

Figure 6. Fold changes of DiART-tagged amine metabolites (n = 5). Metabolites were targeted by comparing retention time and exact mass of DiART-tagged standards. Error bars are SEM; * denotes $p < 0.05$.

Pathway Analysis

A major benefit of untargeted metabolomics is its amenability to discover novel pathway aberrations, which provide insight into disease pathogenesis as well as potential biomarkers and therapeutic targets. Of the 719 targeted and untargeted compounds identified with METLIN, 349 had KEGG IDs, which were input into the metabolomics analysis tool MetPA. MetPA is capable of conducting both pathway enrichment analysis and pathway topological analysis of 874 metabolic pathways.[26] The generated data showed at least 2 metabolite hits in each of 48 pathways (Figure 7a and Table 2), with the most hits for arginine and proline metabolism (14), followed by amino sugar and nucleotide sugar metabolism (13) and galactose metabolism (12). Pathways were also assigned a pathway impact factor, which is calculated by summing importance measures of matched metabolites in the network, with an impact factor of 1 being the maximum. The synthesis and degradation of ketone bodies pathway had the highest impact factor (0.7). Figure 7b shows a simplified schematic of the metabolic pathways listed in Table 2 as well as the number of metabolites changed in each pathway. The map enables visualization of the metabolic connections between each pathway and emphasizes the importance of global metabolic approaches toward understanding the full picture of pathway dysfunction in diabetes.

DISCUSSION

This study demonstrates a novel approach for identifying a diverse group of metabolites in diabetic vascular tissue. The results of this work reveal changes in 48 metabolic pathways, each with at least two metabolites with $p \leq 0.05$ and fold changes ≥2 or ≤0.5. The majority of these are involved in (1) carbonyl stress, (2) carbohydrate metabolism, and/or (3) amino acid metabolism. Propanoate, butanoate, and vitamin B6 metabolism were among the top 20 pathways with the greatest number of altered metabolites. Few studies have examined the involvement of these pathways in diabetic vascular tissue. The implications of these findings in the pathogenesis and as therapeutic targets for diabetic vascular injury are detailed below.

Carbonyl Stress

Diabetic carbonyl stress arises due to a buildup of cytotoxic reactive carbonyl species, particularly α-oxoaldehydes, produced via lipid or glucose degradation.[35] Unregulated lipolysis, characterized by overproduction of free fatty acids (FFAs), is one of the hallmarks of type 2 diabetes.[37] β-Oxidation of these FFAs leads to an increase in acetyl-CoA, which is subsequently converted to ketone bodies (KBs), particularly during TCA cycle overload (discussed below). As shown in Figure 7a,b and Table 2, the pathway for the synthesis and degradation of KBs was ranked the highest impact (0.7) by MetPA pathway topological analysis. While this pathway consists of only six metabolites, it is altered dramatically in diabetic vascular tissue. Although increased production of the three endogenous KBs, acetoacetate (AcAc), 3-hydroxybutyrate (3HB), and acetone, is most often associated with low levels of insulin, as in type 1 diabetes, it has been observed in end-stage type 2 diabetes as well.[38] AcAc and 3HB are present in a 1:1 ratio in nondiabetic individuals, but studies have found 3HB:AcAc levels as high as 10:1 in patients with acute diabetic ketoacidosis.[39] In our study, both 3HB and AcAc were detected with fold changes of 7.48 and 0.37, respectively (Table S2, Supporting Information), indicative of ketoacidosis. Furthermore, the triglyceride breakdown product glycerol was detected in positive mode with a fold change of 15.78, (Table S1, Supporting Information), which is consistent with increased lipolysis. The ketogenic amino acid leucine, which increased 42% in DiART data (Figure 6), respectively, may also contribute to higher levels of acetyl-CoA and thus KBs.[40]

dx.doi.org/10.1021/pr501030e | J. Proteome Res. 2014, 13, 6121−6134

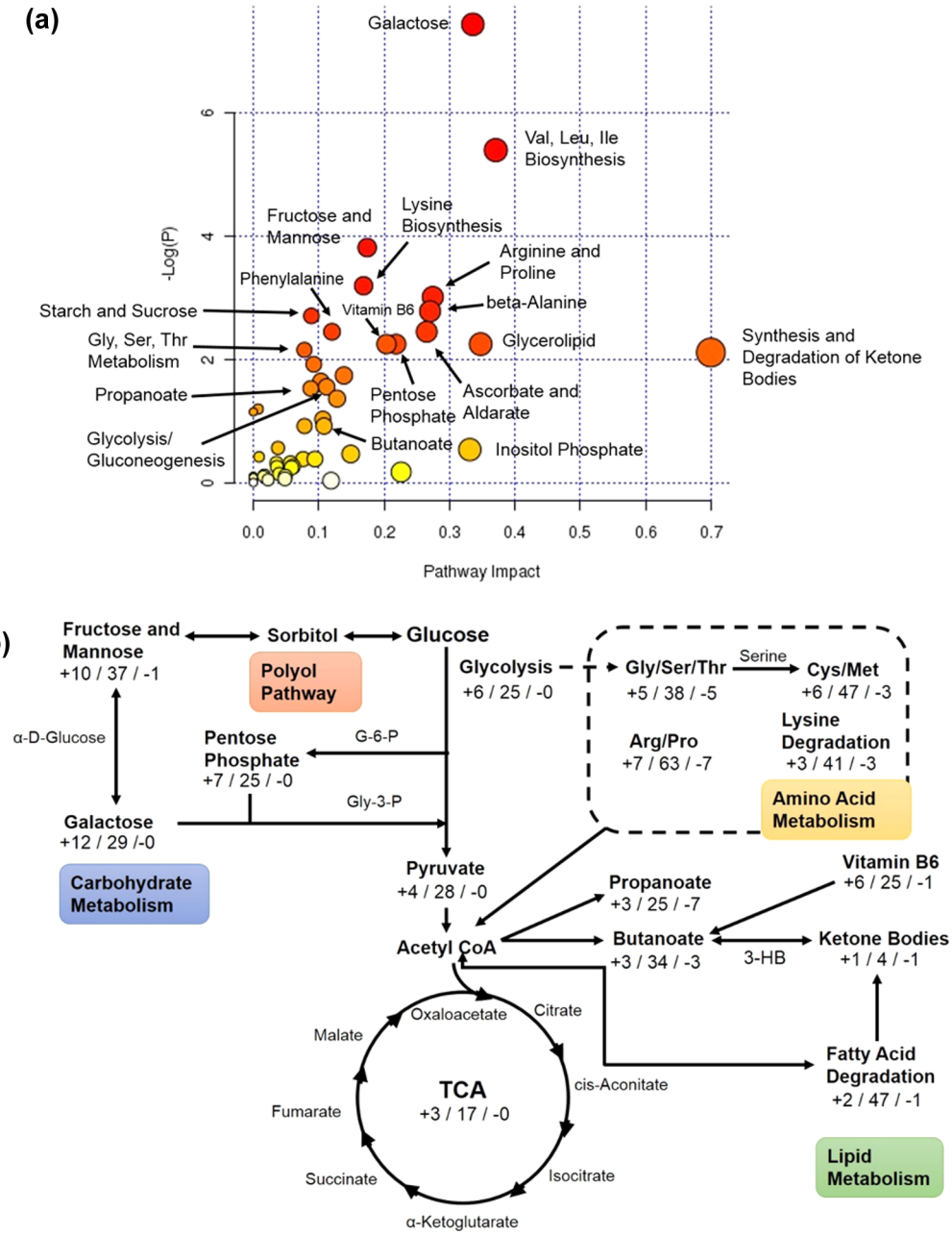

Figure 7. (a) MetPA analysis pathways. Node size and color indicate the degree of importance. Large red nodes are pathways with the highest level of change in diabetes. Orange, yellow, and white nodes represent moderate, slight, and zero importance, respectively. (b) Simplified schematic of some of the pathways identified in MetPA. The notation below each pathway indicates hits in each pathway as the number of increases/number unchanged/number of decreases.

Reactive carbonyls are also capable of reacting nonenzymatically with amino acid residues to form irreversible advanced glycation end products (AGEs) or advanced lipoxidation end products (ALEs). AGEs and ALEs damage cells through several mechanisms, including increased reactive oxygen species production, ultimately leading to an inflammatory response and vascular complications.[41] One of the most prevalent AGEs found in diabetes is methylglyoxal (fold change 2.25), which can be produced from glycolytic intermediates, including glyceraldehyde-3-phosphate (G-3-P), and incidentally also from KBs, which were shown to increase significantly in this study.[35] The polyol pathway has also been shown to contribute to methylglyoxal production (see the Carbohydrate Metabolism section).[1] As found in the targeted carbonyl study illustrated in Figure 5b, both G-3-P and methylglyoxal increased considerably in diabetes, with fold changes of 2.88 and 2.25, respectively. Another reactive carbonyl species of note is malondialdehyde, which is produced by lipid degradation and can exacerbate diabetic complications by cross-linking with collagen, thereby stiffening arterial walls and leading to vascular damage.[42] In this work, malondialdehyde was found to be elevated 51% in diabetes (Figure 5b). Other compounds related to carbonyl stress found in this study include the AGE precursor fructoselysine and the arginine-derived AGE imidazolone;[43] fold changes were 7.11 and 2.81, respectively (Table S1, Supporting Information). All of these findings support the role of carbonyls in diabetic pathogenesis of

dx.doi.org/10.1021/pr501030e | J. Proteome Res. 2014, 13, 6121−6134

Table 2. List of Pathways Found by Qualitative MetPA Analysis[a]

ranking	pathway	total	expected	hits	% found	raw *p*	impact
	(A) Carbonyl Metabolism						
2	metabolism of ketone bodies	6	0.66	2	33.3	1.33×10^{-1}	0.70
	(B) Carbohydrate Metabolism						
3	galactose metabolism	41	4.48	12	29.3	9.68×10^{-4}	0.34
4	fructose and mannose metabolism	48	5.24	11	22.9	1.21×10^{-2}	0.27
5	ascorbate and aldarate metabolism	45	4.92	10	22.2	2.03×10^{-2}	0.28
7	pentose phosphate pathway	32	3.5	7	21.9	5.27×10^{-2}	0.22
12	glycolysis or gluconeogenesis	31	3.39	6	19.4	1.14×10^{-1}	0.21
16	starch and sucrose metabolism	50	5.46	9	18.0	8.80×10^{-2}	0.09
18	pentose and glucuronate interconversions	53	5.79	9	17.0	1.17×10^{-1}	0.14
21	citrate cycle (TCA cycle)	20	2.19	3	15.0	3.76×10^{-1}	0.24
23	amino sugar and nucleotide sugar metabolism	88	9.62	13	14.8	1.57×10^{-1}	0.16
27	pyruvate metabolism	32	3.5	4	12.5	4.69×10^{-1}	0.19
32	inositol phosphate metabolism	39	4.26	4	10.3	6.31×10^{-1}	0.33
33	glyoxylate and dicarboxylate metabolism	50	5.46	5	10.0	6.52×10^{-1}	0.04
	(C) Amino Acid Metabolism						
1	Val, Leu, and Ile biosynthesis	27	2.95	9	33.3	1.53×10^{-3}	0.39
6	Lys biosynthesis	32	3.5	7	21.9	5.27×10^{-2}	0.17
9	*β*-Ala metabolism	28	3.06	6	21.4	7.69×10^{-2}	0.27
10	Gly, Ser, and Thr metabolism	48	5.24	10	20.8	3.10×10^{-2}	0.08
11	Phe metabolism	45	4.92	9	20.0	5.02×10^{-2}	0.12
14	Arg and Pro metabolism	77	8.41	14	18.2	3.59×10^{-2}	0.27
15	D-Gln and D-glutamate metabolism	11	1.2	2	18.2	3.42×10^{-1}	0.00
19	Cys and Met metabolism	56	6.12	9	16.1	1.51×10^{-1}	0.10
22	Phe, Tyr, and Trp biosynthesis	27	2.95	4	14.8	3.40×10^{-1}	0.01
24	Tyr metabolism	76	8.3	11	14.5	2.01×10^{-1}	O.13
25	Lys degradation	47	5.14	6	12.8	4.09×10^{-1}	0.11
26	Val, Leu, and Ile degradation	40	4.37	5	12.5	4.48×10^{-1}	0.08
28	Ala, aspartate, and glutamate metabolism	24	2.62	3	12.5	4.97×10^{-1}	0.06
34	His metabolism	44	4.81	4	9.1	7.25×10^{-1}	0.08
37	glutathione metabolism	38	4.15	3	7.9	8.02×10^{-1}	0.06
39	Trp metabolism	79	8.63	6	7.6	8.79×10^{-1}	0.23
	(D) Propanoate and Butanoate Metabolism						
17	propanoate metabolism	35	3.82	6	17.1	1.76×10^{-1}	0.09
20	butanoate metabolism	40	4.37	6	15.0	2.68×10^{-1}	0.19
	(E) Metabolism of Cofactors and Vitamins						
8	vitamin B6 metabolism	32	3.5	7	21.9	5.27×10^{-2}	0.22
29	nicotinate and nicotinamide metabolism	44	4.81	5	11.4	5.35×10^{-1}	0.09
30	pantothenate and CoA biosynthesis	27	2.95	3	11.1	5.79×10^{-1}	0.06
36	thiamine metabolism	24	2.62	2	8.3	7.56×10^{-1}	0.04
43	ubiquinone and terpenoid-quinone biosynthesis	36	3.93	2	5.6	9.18×10^{-1}	0.05
47	folate biosynthesis	42	4.59	2	4.8	9.54×10^{-1}	0.05
	(F) Lipid Metabolism						
13	glycerolipid metabolism	32	3.5	6	18.8	1.29×10^{-1}	0.35
38	glycerophospholipid metabolism	39	4.26	3	7.7	8.17×10^{-1}	0.01
41	fatty acid metabolism	50	5.46	3	6.0	9.24×10^{-1}	0.02
48	steroid hormone biosynthesis	99	10.82	3	3.0	9.99×10^{-1}	0.00
	(G) Nucleotide Metabolism						
44	purine metabolism	92	10.05	5	5.4	9.79×10^{-1}	0.12
46	pyrimidine metabolism	60	6.56	3	5.0	9.68×10^{-1}	0.02
	(H) Energy Metabolism						
31	sulfur metabolism	18	1.97	2	11.1	6.01×10^{-1}	0.04
42	methane metabolism	34	3.71	2	5.9	9.00×10^{-1}	0.02
45	nitrogen metabolism	39	4.26	2	5.1	9.38×10^{-1}	0.00
	(I) Terpenoid Metabolism						
35	terpenoid backbone biosynthesis	33	3.61	3	9.1	7.17×10^{-1}	0.04
	(J) Translation						
40	aminoacyl-tRNA biosynthesis	75	8.19	5	6.7	9.26×10^{-1}	0.00

[a]Pathways are ranked by percent of compounds found in each pathway, which was determined by dividing the number of hits by the total number of compounds in the pathway. The number of expected compounds was determined by over-representation analysis in MetPA, which uses hypergeometric testing to calculate the number of compounds expected to be in each pathway by chance alone. Raw *p* values were determined on

dx.doi.org/10.1021/pr501030e | J. Proteome Res. 2014, 13, 6121−6134

Table 2. continued

the basis of the number of hits and total number of compounds in the pathway. The pathway impact was found using relative betweenness centrality pathway topology analysis, which calculates metabolite importance measures on the basis of their position in the pathway.

vascular tissue, both via the buildup of KBs and by the formation of AGEs and ALEs.

Carbohydrate Metabolism

As diabetes is defined by chronic hyperglycemia, it follows that carbohydrate metabolism must be altered in order to accommodate the high glucose load. Table 2 shows changes in many pathways related to sugar metabolism, including galactose, starch and sucrose, fructose and mannose, glycolysis, TCA, and pentose phosphate pathways. Galactose metabolism, which had the third-highest percent change of all the pathways found in MetPA, has been associated with increased oxidative stress and microvascular complications.[44] Likewise, fructose and mannose metabolism, which shares four of the compounds found to be altered in galactose metabolism, was ranked fourth by MetPA with 22.92% of the compounds found. One of the compounds found in both galactose and fructose and mannose pathways is sorbitol, which increased 2.55-fold (Table S2, Supporting Information). Sorbitol is also produced in the polyol pathway, which is classified as part of the fructose and mannose pathway in KEGG. In the polyol pathway, glucose is reduced to sorbitol via aldose reductase, which simultaneously oxidizes NADPH to $NADP^+$; sorbitol is then converted to fructose by sorbitol dehydrogenase. The buildup of sorbitol can cause osmotic stress as well as AGE formation, and lower levels of NADPH lead to NO and glutathione deficiencies, which promote oxidative stress.[1] Although polyol pathway dysfunction appears to play a major role in diabetic vascular damage, over 20 clinical trials using drugs targeting aldose reductase and sorbitol dehydrogenase have failed to ameliorate these complications.[45,46] Research in this area is further compounded by the tissue-specific influence of the polyol pathway on oxidative damage[47,48] but continues to hold some promise for understanding the mechanisms of diabetic complications.

Because glucose is a direct substrate for glycolysis, both glycolysis and the downstream TCA cycle were selected for targeted analysis (Figure 4). As detailed in the Results section, the first eight targeted metabolites increased in diabetes (six with $p < 0.05$), and the remainder of the TCA cycle—succinate, fumarate, and malate—showed small fold changes and no statistical significance. The rate-limiting step, which determines metabolic flux through the TCA cycle, is the conversion of α-ketoglutarate to succinate via α-ketoglutarate dehydrogenase.[49] α-Ketoglutarate dehydrogenase and aconitase, which converts citrate to isocitrate, are inhibited by reactive oxygen species, leading to metabolic deficiency in the rest of the cycle.[50] α-Ketoglutarate dehydrogenase or aconitase dysfunction may be responsible for the halting of significant elevation in later TCA metabolites. Further isotope flux analyses are needed to evaluate this phenomenon.

The pentose phosphate pathway (PPP), an offshoot of glycolysis (Figure 7b), was also found to be elevated. Six metabolites from the PPP—G-6-P, β-D-glucose, gluconic acid, 2-dehydro-3-deoxy-D-gluconate, pyruvate, and glyceric acid—were detected and elevated in diabetic tissue. Since PPP activation is dependent on G-6-P levels, the elevation/activation is expected.

Vitamin B6 Metabolism

The most biologically active form of vitamin B6, pyridoxal phosphate (PLP), is an important cofactor in several enzymatic reactions, including carbohydrate and amino acid metabolism.[51] Deficiencies of PLP are associated with abnormal glucose tolerance, risk of stroke, and diabetes.[52] MetPA analysis showed seven hits, or 21.9% of compounds involved in PLP catabolism, to be significantly altered in diabetic aorta (Table 2). Of these, six of the seven (4- and 5-pyridoxolactone, pyruvate, α-ketoglutarate, 2-methyl-3-hydroxy-5-formylpyridine-4-carboxylate, and 4-pyridoxic acid) were found to be up-regulated. With the exception of the TCA cycle metabolites α-ketoglutarate and pyruvate, the remainder of the metabolites are exclusive to the PLP pathway. Notably, the end product of pyridoxal oxidation, 4-pyridoxic acid, increased 3-fold (Table S7, Supporting Information), suggesting substantial PLP degradation.[52] Some work suggests that PLP supplementation has therapeutic potential in managing diabetic neuropathy,[53] but these benefits have yet to be studied in diabetic vascular tissue.

Because of its important role as a cofactor in amino acid catabolism, the dysfunction of the PLP pathway is likely connected with aberrant amino acid metabolism.[51] The tryptophan metabolites kynurenine (Kyn) and 3-hydroxykynurenine were detected in the carbonyl tagging study at fold changes of 5.84 and 2.72, respectively (Table S3, Supporting Information). These findings are consistent with other work that showed increases in tryptophan metabolites as a result of the decreased activity of the PLP-dependent enzyme kynureninase,[54] which is involved in their catabolism. As Kyn metabolites are known to inhibit insulin secretion and reduce glucose tolerance,[51] PLP deficiency may exacerbate diabetic complications both via the buildup of reactive oxygen species and by preventing effective degradation of tryptophan. We hypothesize that the interactions of PLP and Trp-Kyn metabolism may be a therapeutic route for ameliorating oxidative stress in diabetes. Future targeted LC–MS studies may allow for a more thorough investigation of vitamin B6 metabolism in diabetic aorta.

Propanoate and Butanoate Metabolism

Despite limited reports in diabetes literature,[48] the fact that many of the metabolic intermediates in the propanoate and butanoate pathways (20% and 15% of compounds found, respectively; Tables S8 and S9, Supporting Information) are present in other pathways as well (Figure 7b) is an indication of the importance of these pathways to the overall picture of diabetic metabolic dysfunction. For example, the ketone body AcAc (discussed in the Carbonyl Stress section) is involved in both propanoate and butanoate metabolism; the second major ketone body 3-HB participates in the butanoate pathway. As shown in Table S8 (Supporting Information), despite the slight increase in valine, which is an edge node for the propanoate pathway, all of the other compounds decrease with the exception of malonic semialdehyde and hydroxybutyrate. Malonic semialdehyde is also involved in β-alanine metabolism, another pathway found to be significantly changed in MetPA analysis. It produces acetyl-CoA in the propanoate pathway, and its increase, along with unregulated lipolysis, likely contributes to the synthesis of KBs (discussed in the Carbonyl

dx.doi.org/10.1021/pr501030e | J. Proteome Res. 2014, 13, 6121–6134

Stress section). Six compounds involved in butanoate metabolism were found in this study (Table S9, Supporting Information). As shown in Figure 7b, because the butanoate pathway is centrally positioned between pathways involved in lipid, carbohydrate, and amino acid metabolism, compounds in the butanoate pathway may be affected by dysregulation in several other metabolic pathways. For instance, both α-ketoglutarate and succinate participate in the TCA cycle (see Carbohydrate Metabolism), and succinic acid semialdehyde, which decreased 63%, is linked to the metabolism of several amino acids, including glutamate and tyrosine.[55]

Although gene expression studies have implicated the propanoate pathway in the pathogenesis of diabetic nephropathy,[56] to our knowledge this is the first report of propanoate and butanoate metabolic irregularities in diabetic vascular tissue. We hypothesize that the down-regulation we discovered in propanoate and butanoate metabolism may be connected to dyslipidemia as well as insulin resistance. Short-chain fatty acids including propanoate and butanoate have recently been shown to reduce food intake and protect against diet-induced obesity in FFA-receptor-deficient mice.[57] Other studies have examined short-chain fatty acid supplementation as a means to regulate blood glucose levels, inhibit cholesterol synthesis, and improve carbohydrate metabolism.[58] While these findings have shown some promise, the application of propanoate and butanoate pathway regulation as a therapeutic route for diabetic vascular complications remains to be demonstrated.

Amino Acid Metabolism

Diabetes risk is associated with aberrant metabolism of the branched-chain amino acids valine, leucine, and isoleucine, which have been shown to contribute to insulin resistance.[10] The highest-ranking amino acid pathway found by MetPA (Table 2) is valine, leucine, and isoleucine biosynthesis. While this biosynthesis pathway does not occur in humans, valine, leucine, and isoleucine degradation pathways are available. The elevation in biosynthesis is due to the overlap between the biosynthesis and degradation pathways of these particular amino acids, as well as the ability of humans to partially biosynthesize them. For the purposes of this discussion, only degradation pathways are considered.

The branched chain amino acids play many roles in cellular function, such as protein and lipid synthesis and cellular growth.[40] Studies show a positive correlation between insulin resistance and levels of these amino acids, and thus they are used as biomarkers in predicting diabetes progression.[59] Table 2 shows that 12.5% of the compounds in valine, leucine, and isoleucine degradation was significantly changed, including elevations in all three amino acids (with $p < 0.05$ for valine and leucine, Figure 6). The other compounds found are methyl malonate, methyl malonic acid semialdehyde, and acetoacetate, all of which are also involved in propanoate metabolism, as previously discussed.

The relationship between lysine degradation and diabetes has yet to be fully understood, although studies suggest that lysine is relevant to diabetes.[17,60] MetPA analysis showed six hits (12.8% of compounds) in the lysine degradation pathway. Carnitine, an end product of lysine degradation that is also involved in β-oxidation of fatty acids, was found to increase 3.9-fold. The health effects of carnitine are currently under debate, and several clinical trials have shown a link between carnitine and diabetic complications.[61,62]

Metabolism of the aromatic amino acids tryptophan, tyrosine, and phenylalanine was also found to be disrupted, with 14.8% of compounds altered in their biosynthesis. Tryptophan is associated with increased food intake in diabetes.[63] Not surprisingly, MetPA analysis revealed the greatest change through the part of the tryptophan degradation pathway that produces acetyl-CoA (hydroxykynurenine, fold change 2.72; aminomuconic acid semialdehyde, fold change 6.17; and kynurenine, fold change 5.84), which, as previously discussed, is involved in many other metabolic pathways such as KB synthesis and the TCA cycle. Tyrosine, which is produced from phenylalanine either enzymatically via phenylalanine hydroxylase or through nonenzymatic oxidation by free radicals, increased 51% in diabetes (Figure 6).

The most MetPA hits (14) out of all the pathways were found in arginine and proline metabolism. Arginine levels are depleted in diabetes, possibly due to glycation of arginine residues in AGE formation.[64] It is also a precursor in NO synthesis and thus plays an important role in vasodilation, although the underlying mechanism remains unclear. Most of the compounds involved in arginine metabolism decreased as expected (e.g., γ-glutamyl-L-putrescine, fold change 0.29; agmatine, fold change 0.19; spermidine, fold change 0.48; and spermine, fold change 0.34), but putrescine, a polyamine involved in diabetic hypertrophy of the kidney,[65] increased 3.18-fold.

CONCLUSION

Diabetes is a debilitating and complex disorder marked by alterations to a host of metabolic pathways as well as underlying biochemical processes, including AGE formation and oxidative stress. The field of metabolomics has made considerable progress toward understanding diabetic pathogenesis but remains inhibited by sensitivity, selectivity, and identification of relevant species of interest. Here we demonstrated the application of two different isobaric tags to improve signal and identification of amines and carbonyls in diabetic vascular tissue. A global metabolomic study was also conducted to identify other compounds that change in diabetes. A tremendous number of spectral features were uncovered in this work, 1.3% of which were identified following data processing. Importantly, many of the unidentified compounds may be undiscovered or uncharacterized metabolites that have yet to be described in database libraries. Continued expansion of these databases would almost certainly allow for the identification of more compounds in future studies.

The findings presented here give credence to the notion that biomarkers and individual compounds provide only part of the overall story of diabetic metabolic dysfunction. Pathway analysis, especially on a group of diverse metabolites with roles ranging from carbohydrate to amino acid metabolism, can shed light on underlying mechanisms and interplay between metabolic networks that would otherwise remain undiscovered. For example, few reports have described the role of butanoate, propanoate, and vitamin B6 metabolism in diabetic complications, but these pathways were among the most substantially changed in this study. Future experiments that build on this work include isotope flux analysis and human tissue research, which would provide more insight into the roles of various metabolic and nonmetabolic pathways in diabetic vascular complications.

■ ASSOCIATED CONTENT

Supporting Information

Table S1, an Excel file listing identified untargeted positive mode metabolites (metabolites highlighted in blue are biomarkers of oxidative stress and those highlighted in yellow have MS/MS fragmentation patterns that match standards in METLIN); Table S2, an Excel file listing identified untargeted negative mode metabolites (metabolites highlighted in yellow have MS/MS fragmentation patterns that match standards in METLIN); Table S3, an Excel file listing identified carbonyl increases; Table S4, an Excel file listing identified carbonyl decreases; Table S5, an Excel file listing identified oxidized carbonyl increases found in MCID; and Table S6, an Excel file listing identified oxidized carbonyl decreases found in MCID; and a pdf file that includes Table S7, a list of vitamin B6 pathway significant changes; Table S8, a list of propanoate pathway significant changes; Table S9, a list of butanoate pathway significant changes. This material is available free of charge via the Internet at http://pubs.acs.org.

■ AUTHOR INFORMATION

Corresponding Author

*Phone +1 314 977 3624. Fax: 314-977-2521. E-mail: jedward5@slu.edu.

Author Contributions

⊥L.A.F. and W.Y. contributed equally.

Notes

The authors declare no competing financial interest.

■ ACKNOWLEDGMENTS

This work was supported by the American Heart Association (JLE, 10SDG3640026) and National Institutes of Health (ELF, 1DP3DK094292 and R24 082841).

■ REFERENCES

(1) Giacco, F.; Brownlee, M. Oxidative stress and diabetic complications. *Circ. Res.* **2010**, *107* (9), 1058−1070.

(2) Kaiser, N.; Sasson, S.; Feener, E. P.; Boukobza-Vardi, N.; Higashi, S.; Moller, D. E.; Davidheiser, S.; Przybylski, R. J.; King, G. L. Differential regulation of glucose transport and transporters by glucose in vascular endothelial and smooth muscle cells. *Diabetes* **1993**, *42* (1), 80−9.

(3) Setter, S. M.; Campbell, R. K.; Cahoon, C. J. Biochemical pathways for microvascular complications of diabetes mellitus. *Ann. Pharmacother.* **2003**, *37*, 1858−1866.

(4) Natorska, J.; Wypasek, E.; Grudzień, G.; Sobczyk, D.; Marek, G.; Filip, G.; Sadowski, J.; Undas, A. Does diabetes accelerate the progression of aortic stenosis through enhanced inflammatory response within aortic valves? *Inflammation* **2012**, *35* (3), 834−840.

(5) Scott, L. J.; Mohlke, K. L.; Bonnycastle, L. L.; Willer, C. J.; Li, Y.; Duren, W. L.; Erdos, M. R.; Stringham, H. M.; Chines, P. S.; Jackson, A. U.; Prokunina-Olsson, L.; Ding, C.-J.; Swift, A. J.; Narisu, N.; Hu, T.; Pruim, R.; Xiao, R.; Li, X.-Y.; Conneely, K. N.; Riebow, N. L.; Sprau, A. G.; Tong, M.; White, P. P.; Hetrick, K. N.; Barnhart, M. W.; Bark, C. W.; Goldstein, J. L.; Watkins, L.; Xiang, F.; Saramies, J.; Buchanan, T. A.; Watanabe, R. M.; Valle, T. T.; Kinnunen, L.; Abecasis, G. R.; Pugh, E. W.; Doheny, K. F.; Bergman, R. N.; Tuomilehto, J.; Collins, F. S.; Boehnke, M. A genome-wide association study of type 2 diabetes in finns detects multiple susceptibility variants. *Science* **2007**, *316* (5829), 1341−1345.

(6) Raamsdonk, L. M.; Teusink, B.; Broadhurst, D.; Zhang, N.; Hayes, A.; Walsh, M. C.; Berden, J. A.; Brindle, K. M.; Kell, D. B.; Rowland, J. J.; Westerhoff, H. V.; van Dam, K.; Oliver, S. G. A functional genomics strategy that uses metabolome data to reveal the phenotype of silent mutations. *Nat. Biotechnol.* **2001**, *19* (1), 45−50.

(7) Ahmed, M.; Forsberg, J.; Bergsten, P. Protein profiling of human pancreatic islets by two-dimensional gel electrophoresis and mass spectrometry. *J. Proteome Res.* **2005**, *4* (3), 931−940.

(8) Wang, C.; Kong, H.; Guan, Y.; Yang, J.; Gu, J.; Yang, S.; Xu, G. Plasma phospholipid metabolic profiling and biomarkers of type 2 diabetes mellitus based on high-performance liquid chromatography/electrospray mass spectrometry and multivariate statistical analysis. *Anal. Chem.* **2005**, *77* (13), 4108−4116.

(9) Zhang, H.; Saha, J.; Byun, J.; Schin, M.; Lorenz, M.; Kennedy, R. T.; Kretzler, M.; Feldman, E. L.; Pennathur, S.; Brosius, F. C., 3rd. Rosiglitazone reduces renal and plasma markers of oxidative injury and reverses urinary metabolite abnormalities in the amelioration of diabetic nephropathy. *Am. J. Physiol. Renal Physiol.* **2008**, *295* (4), F1071−81.

(10) Newgard, C. B.; An, J.; Bain, J. R.; Muehlbauer, M. J.; Stevens, R. D.; Lien, L. F.; Haqq, A. M.; Shah, S. H.; Arlotto, M.; Slentz, C. A.; Rochon, J.; Gallup, D.; Ilkayeva, O.; Wenner, B. R.; Yancy, W. S., Jr.; Eisenson, H.; Musante, G.; Surwit, R. S.; Millington, D. S.; Butler, M. D.; Svetkey, L. P. A branched-chain amino acid-related metabolic signature that differentiates obese and lean humans and contributes to insulin resistance. *Cell Metab.* **2009**, *9* (4), 311−326.

(11) Xu, F.; Tavintharan, S.; Sum, C. F.; Woon, K.; Lim, S. C.; Ong, C. N. Metabolic signature shift in type 2 diabetes mellitus revealed by mass spectrometry-based metabolomics. *J. Clin. Endocrinol. Metab.* **2013**, *98* (6), E1060−E1065.

(12) Ashrafian, H.; Li, J. V.; Spagou, K.; Harling, L.; Masson, P.; Darzi, A.; Nicholson, J. K.; Holmes, E.; Athanasiou, T. Bariatric surgery modulates circulating and cardiac metabolites. *J. Proteome Res.* **2014**, *13*, 570−580.

(13) Fardet, A.; Llorach, R.; Martin, J.-F. o.; Besson, C.; Lyan, B.; Pujos-Guillot, E.; Scalbert, A. A liquid chromatography−quadrupole time-of-flight (LC−QTOF)-based metabolomic approach reveals new metabolic effects of catechin in rats fed high-fat diets. *J. Proteome Res.* **2008**, *7* (6), 2388−2398.

(14) Yuan, W.; Edwards, J. L. Thiol metabolomics of endothelial cells using capillary liquid chromatography mass spectrometry with isotope coded affinity tags. *J. Chromatogr., A* **2011**, *1218* (18), 2561−2568.

(15) Yuan, W.; Edwards, J. L.; Li, S. Global profiling of carbonyl metabolites with a photo-cleavable isobaric labeling affinity tag. *Chem. Commun.* **2013**, *49* (94), 11080−11082.

(16) Baynes, J. W.; Thorpe, S. R. Role of oxidative stress in diabetic complications: A new perspective on an old paradigm. *Diabetes* **1999**, *48* (1), 1−9.

(17) Yuan, W.; Zhang§, J.; Li, S.; Edwards, J. L. Amine metabolomics of hyperglycemic endothelial cells using capillary LC−MS with isobaric tagging. *J. Proteome Res.* **2011**, *10* (11), 5242−5250.

(18) Yuan, W.; Edwards, J. L. Capillary separations in metabolomics. *Bioanalysis* **2010**, *2* (5), 953−963.

(19) Zhang, J.; Wang, Y.; Li, S. Deuterium isobaric amine-reactive tags for quantitative proteomics. *Anal. Chem.* **2010**, *82* (18), 7588−95.

(20) Sullivan, K. A.; Hayes, J. M.; Wiggin, T. D.; Backus, C.; Su Oh, S.; Lentz, S. I.; Brosius, F., III; Feldman, E. L. Mouse models of diabetic neuropathy. *Neurobiol. Dis.* **2007**, *28* (3), 276−285.

(21) Kobayashi, M.; Inoue, K.; Warabi, E.; Minami, T.; Kodama, T. A simple method of isolating mouse aortic endothelial cells. *J. Atheroscler. Thromb.* **2005**, *12* (3), 138−42.

(22) Tautenhahn, R.; Patti, G. J.; Rinehart, D.; Siuzdak, G. XCMS online: A Web-based platform to process untargeted metabolomic data. *Anal. Chem.* **2012**, *84* (11), 5035−5039.

(23) Smith, C. A.; O'Maille, G.; Want, E. J.; Qin, C.; Trauger, S. A.; Brandon, T. R.; Custodio, D. E.; Abagyan, R.; Siuzdak, G. METLIN: A metabolite mass spectral database. *Ther. Drug Monit.* **2005**, *27*, 747−751.

(24) Wishart, D. S.; Tzur, D.; Knox, C.; Eisner, R.; Guo, A. C.; Young, N.; Cheng, D.; Jewell, K.; Arndt, D.; Sawhney, S.; Fung, C.; Nikolai, L.; Lewis, M.; Coutouly, M. A.; Forsythe, I.; Tang, P.; Shrivastava, S.; Jeroncic, K.; Stothard, P.; Amegbey, G.; Block, D.; Hau,

D. D.; Wagner, J.; Miniaci, J.; Clements, M.; Gebremedhin, M.; Guo, N.; Zhang, Y.; Duggan, G. E.; Macinnis, G. D.; Weljie, A. M.; Dowlatabadi, R.; Bamforth, F.; Clive, D.; Greiner, R.; Li, L.; Marrie, T.; Sykes, B. D.; Vogel, H. J.; Querengesser, L. HMDB: The human metabolome database. *Nucleic Acids Res.* **2007**, *35* (Database issue), D521−6.

(25) Kanehisa, M.; Goto, S.; Sato, Y.; Kawashima, M.; Furumichi, M.; Tanabe, M. Data, information, knowledge and principle: Back to metabolism in KEGG. *Nucleic Acids Res.* **2014**, *42*.

(26) Xia, J.; Wishart, D. S. MetPA: A Web-based metabolomics tool for pathway analysis and visualization. *Bioinformatics* **2010**, *26* (18), 2342−2344.

(27) Li, L.; Li, R.; Zhou, J.; Zuniga, A.; Stanislaus, A. E.; Wu, Y.; Huan, T.; Zheng, J.; Shi, Y.; Wishart, D. S.; Lin, G. MyCompoundID: Using an evidence-based metabolome library for metabolite identification. *Anal. Chem.* **2013**, *85* (6), 3401−3408.

(28) Tojo, G.; Fernandez, M. *Oxidation of Alcohols to Aldehydes and Ketones: A Guide to Current Common Practice*; Springer: New York, 2006.

(29) Roberts, L. D.; Koulman, A.; Griffin, J. L. Towards metabolic biomarkers of insulin resistance and type 2 diabetes: Progress from the metabolome. *Lancet Diabetes Endocrinol.* **2014**, *2* (1), 65−75.

(30) Bictash, M.; Ebbels, T. M.; Chan, Q.; Loo, R. L.; Yap, I. K. S.; Brown, I. J.; de Iorio, M.; Daviglus, M. L.; Holmes, E.; Stamler, J.; Nicholson, J. K.; Elliott, P. Opening up the "black box": Metabolic phenotyping and metabolome-wide association studies in epidemiology. *J. Clin. Epidemiol.* **2010**, *63* (9), 970−979.

(31) Patti, G. J.; Tautenhahn, R.; Rinehart, D.; Cho, K.; Shriver, L. P.; Manchester, M.; Nikolskiy, I.; Johnson, C. H.; Mahieu, N. G.; Siuzdak, G. A view from above: Cloud plots to visualize global metabolomic data. *Anal. Chem.* **2012**, *85* (2), 798−804.

(32) Patti, G. J.; Tautenhahn, R.; Siuzdak, G. Meta-analysis of untargeted metabolomic data from multiple profiling experiments. *Nat. Protocols* **2012**, *7* (3), 508−516.

(33) Perreault, H.; Lattova, E.; Sagi, D.; Peter-Katalinic, J. MALDI-MS of glycans and glycoconjugates. In *MALDI MS: A Practical Guide to Instrumentation, Methods and Applications*, 2nd ed.; Hillenkamp, F., Peter-Katalinic, J., Eds.; Wiley-Blackwell: Weinheim, Germany, 2013; p 258.

(34) Siuzdak, G. METLIN: Metabolite and tandem MS database. http://metlin.scripps.edu/index.php (accessed June 17, 2014).

(35) Turk, Z. Glycotoxines, carbonyl stress and relevance to diabetes and its complications. *Physiol. Res.* **2010**, *59*, 147−156.

(36) Backwell, F. R. C. Peptide utilization by tissues: Current status and applications of stable isotope procedures. *Proc. Nutr. Soc.* **1994**, *53*, 457−464.

(37) McGarry, J. D. Banting lecture 2001: Dysregulation of fatty acid metabolism in the etiology of type 2 diabetes. *Diabetes* **2002**, *51* (1), 7−18.

(38) Mahendran, Y.; Vangipurapu, J.; Cederberg, H.; Stančáková, A.; Pihlajamäki, J.; Soininen, P.; Kangas, A. J.; Paananen, J.; Civelek, M.; Saleem, N. K.; Pajukanta, P.; Lusis, A. J.; Bonnycastle, L. L.; Morken, M. A.; Collins, F. S.; Mohlke, K. L.; Boehnke, M.; Ala-Korpela, M.; Kuusisto, J.; Laakso, M. Association of ketone body levels with hyperglycemia and type 2 diabetes in 9,398 Finnish men. *Diabetes* **2013**, *62* (10), 3618−3626.

(39) Laffel, L. Ketone bodies: A review of physiology, pathophysiology and application of monitoring to diabetes. *Diabetes Metab. Res. Rev.* **1999**, *15* (6), 412−26.

(40) Hutson, S. M.; Sweatt, A. J.; LaNoue, K. F. Branched-chain amino acid metabolism: Implications for establishing safe intakes. *J. Nutr.* **2005**, *135* (6), 1557S−1564S.

(41) Zhang, Q.; Ames, J. M.; Smith, R. D.; Baynes, J. W.; Metz, T. O. A perspective on the Maillard reaction and the analysis of protein glycation by mass spectrometry: Probing the pathogenesis of chronic disease. *J. Proteome Res.* **2008**, *8* (2), 754−769.

(42) Slatter, D. A.; Bolton, C. H.; Bailey, A. J. The importance of lipid-derived malondialdehyde in diabetes mellitus. *Diabetologia* **2000**, *43* (5), 550−557.

(43) Miyata, T.; de Strihou, C. V.; Kurokawa, K.; Baynes, J. W. Alterations in nonenzymatic biochemistry in uremia: Origin and significance of "carbonyl stress" in long-term uremic complications. *Kidney Int.* **1999**, *55* (2), 389−399.

(44) Kowluru, R. A.; Tang, J.; Kern, T. S. Abnormalities of retinal metabolism in diabetes and experimental galactosemia: VII. Effect of long-term administration of antioxidants on the development of retinopathy. *Diabetes* **2001**, *50* (8), 1938−1942.

(45) Schmidt, R. E.; Dorsey, D. A.; Beaudet, L. N.; Parvin, C. A.; Yarasheski, K. E.; Smith, S. R.; Williamson, J. R.; Peterson, R. G.; Oates, P. J. A potent sorbitol dehydrogenase inhibitor exacerbates sympathetic autonomic neuropathy in rats with streptozotocin-induced diabetes. *Exp. Neurol.* **2005**, *192* (2), 407−19.

(46) Chalk, C.; Benstead, T. J.; Moore, F. Aldose reductase inhibitors for the treatment of diabetic polyneuropathy. *Cochrane Database Syst. Rev.* **2007**, No. 4, Cd004572.

(47) Chung, S. S. M.; Ho, E. C. M.; Lam, K. S. L.; Chung, S. K. Contribution of polyol pathway to diabetes-induced oxidative stress. *J. Am. Soc. Nephrol.* **2003**, *14* (suppl 3), S233−S236.

(48) Zhang, L.; Yu, C.; Vasquez, F. E.; Galeva, N.; Onyango, I.; Swerdlow, R. H.; Dobrowsky, R. T. Hyperglycemia alters the Schwann cell mitochondrial proteome and decreases coupled respiration in the absence of superoxide production. *J. Proteome Res.* **2009**, *9* (1), 458−471.

(49) Fahien, L. A.; MacDonald, M. J. The succinate mechanism of insulin release. *Diabetes* **2002**, *51* (9), 2669−2676.

(50) Vincent, A. M.; Mclean, L. L.; Backus, C.; Feldman, E. L. Short-term hyperglycemia produces oxidative damage and apoptosis in neurons. *FASEB J.* **2005**, *19* (6), 638−640.

(51) Mooney, S.; Leuendorf, J.-E.; Hendrickson, C.; Hellmann, H. Vitamin B6: A long known compound of surprising complexity. *Molecules* **2009**, *14* (1), 329−351.

(52) Rogers, K. S.; Mohan, C. Vitamin B6 metabolism and diabetes. *Biochem. Med. Metab. Biology* **1994**, *52* (1), 10−17.

(53) Nakamura, S.; Li, H.; Adijiang, A.; Pischetsrieder, M.; Niwa, T. Pyridoxal phosphate prevents progression of diabetic nephropathy. *Nephrol., Dial., Transplant.* **2007**, *22* (8), 2165−2174.

(54) Bender, D. A.; Njagi, E. N. M.; Danielian, P. S. Tryptophan metabolism in vitamin B6-deficient mice. *Br. J. Nutr.* **1990**, *63* (01), 27−36.

(55) Gibson, K. M.; Gupta, M.; Pearl, P. L.; Tuchman, M.; Vezina, L. G.; Snead Iii, O. C.; Smit, L. M. E.; Jakobs, C. Significant behavioral disturbances in succinic semialdehyde dehydrogenase (SSADH) deficiency (gamma-hydroxybutyric aciduria). *Biol. Psychiatry* **2003**, *54* (7), 763−768.

(56) Huang, C.; Kim, Y.; Caramori, M. L.; Moore, J. H.; Rich, S. S.; Mychaleckyj, J. C.; Walker, P. C.; Mauer, M. Diabetic nephropathy is associated with gene expression levels of oxidative phosphorylation and related pathways. *Diabetes* **2006**, *55* (6), 1826−1831.

(57) Lin, H. V.; Frassetto, A.; Kowalik, E. J., Jr; Nawrocki, A. R.; Lu, M. M.; Kosinski, J. R.; Hubert, J. A.; Szeto, D.; Yao, X.; Forrest, G.; Marsh, D. J. Butyrate and propionate protect against diet-induced obesity and regulate gut hormones via free fatty acid receptor 3-independent mechanisms. *PLoS One* **2012**, *7* (4), e35240.

(58) Todesco, T.; Rao, A. V.; Bosello, O.; Jenkins, D. J. Propionate lowers blood glucose and alters lipid metabolism in healthy subjects. *Am. J. Clin. Nutr.* **1991**, *54* (5), 860−5.

(59) Connell, T. The complex role of branched chain amino acids in diabetes and cancer. *Metabolites* **2013**, *3* (4), 931−945.

(60) Sulochana, K. N.; Punitham, R.; Ramakrishnan, S. Beneficial effect of lysine and amino acids on cataractogenesis in experimental diabetes through possible antiglycation of lens proteins. *Exp. Eye Res.* **1998**, *67* (5), 597−601.

(61) Koeth, R. A.; Wang, Z.; Levison, B. S.; Buffa, J. A.; Org, E.; Sheehy, B. T.; Britt, E. B.; Fu, X.; Wu, Y.; Li, L.; Smith, J. D.; DiDonato, J. A.; Chen, J.; Li, H.; Wu, G. D.; Lewis, J. D.; Warrier, M.; Brown, J. M.; Krauss, R. M.; Tang, W. H.; Bushman, F. D.; Lusis, A. J.; Hazen, S. L. Intestinal microbiota metabolism of L-carnitine, a nutrient

in red meat, promotes atherosclerosis. *Nat. Med.* **2013**, *19* (5), 576−85.
(62) Stevens, M. J.; Lattimer, S. A.; Feldman, E. L.; Helton, E. D.; Millington, D. S.; Sima, A. A.; Greene, D. A. Acetyl-L-carnitine deficiency as a cause of altered nerve myo-inositol content, Na,K-ATPase activity, and motor conduction velocity in the streptozotocin-diabetic rat. *Metabolism* **1996**, *45* (7), 865−72.
(63) Tormo, M. A.; de Tejada, A. R.; Morales, I.; Paredes, S.; Sánchez, S.; Barriga, C.; Hernández, R. Orally administered tryptophan and experimental type 2 diabetes. *Mol. Cell. Biochem.* **2004**, *261* (1), 57−61.
(64) Goldin, A.; Beckman, J. A.; Schmidt, A. M.; Creager, M. A. Advanced glycation end products: sparking the development of diabetic vascular injury. *Circulation* **2006**, *114* (6), 597−605.
(65) Deng, A.; Munger, K. A.; Valdivielso, J. M.; Satriano, J.; Lortie, M.; Blantz, R. C.; Thomson, S. C. Increased expression of ornithine decarboxylase in distal tubules of early diabetic rat kidneys: Are polyamines paracrine hypertrophic factors? *Diabetes* **2003**, *52* (5), 1235−1239.